Study on the difference in subcooling flow boiling of materials in a vertical rectangular channel at a low flow rate

He, Sihong; Zhao, Jiyun

Published in:
Journal of Physics: Conference Series

Published: 01/01/2024

Document Version:
Final Published version, also known as Publisher's PDF, Publisher's Final version or Version of Record

Published version (DOI):
10.1088/1742-6596/2766/1/012118

Publication details:
He, S., & Zhao, J. (2024). Study on the difference in subcooling flow boiling of materials in a vertical rectangular channel at a low flow rate. *Journal of Physics: Conference Series*, *2766*, Article 012118. https://doi.org/10.1088/1742-6596/2766/1/012118

Study on the difference in subcooling flow boiling of materials in a vertical rectangular channel at a low flow rate

Journal of Physics: Conference Series **2766** (2024) 012118 doi:10.1088/1742-6596/2766/1/012118

Study on the difference in subcooling flow boiling of materials in a vertical rectangular channel at a low flow rate

Sihong He and Jiyun Zhao

Department of Mechanical Engineering, City University of Hong Kong, Tat Chee Avenue, Kowloon Tong, Hong Kong SAR, China

E-mail: jiyuzhao@cityu.edu.hk

Abstract. Alloy materials with excellent properties are widely used in different industrial fields. Conducting flow boiling studies on alloy surfaces will help explore their applications in flow boiling, especially in heat exchange equipment. Five alloys were selected, including 304SS, Inconel600, Monel400, Zr4 and FeCrAl. Bubble dynamics in a vertically upward-flowing rectangular channel were observed using a high-speed camera under the condition of atmospheric pressure, 400 kg·m^-2·s^-1 mass flowrate and 5 K inlet subcooling. Results show that roughness and wettability cannot individually define material-sensitive heat transfer coefficient (HTC) and critical heat flux (CHF). Thermal effusivity shows a linear relationship to HTC. Material-sensitive CHF seems to be a power-law function of the nondimensional parameter of the product of the maximum nucleation site density and the minimum bubble nucleation area.

1. Introduction

The effect of varying surface parameters on boiling performance, such as wettability, roughness, and porosity, has been dug out to facilitate the design of innovative surfaces for highly efficient heat removal [1-3]. However, for large-scale industrial applications, it seems uneconomical and unreliable to modify the alloy surface significantly since it will reduce the excellent corrosion resistance of the alloy itself. Therefore, it has practical engineering and research values to study the boring performance of original alloy surfaces.

In early research, surface roughness and material effusivity were two important factors affecting subcooled flow boiling curves at low pressures and flow rates [4]. However, only a few material parameters were considered, making it difficult to observe the relationship between materials and flow boiling performance. Lee S K conducted extensive experimental work identifying potential connections between materials and flow boiling performance, particularly for critical heat flux (CHF). The surface thermal economy of materials dominates the CHF difference in FeCrAl, Zr4, and Inconel600 at 300 kg·m^-2·s^-1 mass flowrate and high inlet subcooling, namely the synthetical effect of density, specific heat capacity and thermal conductivity [5]. To further explore the influence of flowrate on material-sensitive CHF and heat transfer coefficient (HTC), Lee S K tested 60 test tubes fabricated by seven materials and collected 110 CHF data [6]. The effect of materials on CHF is significant at a relatively low flowrate but is suppressed at higher flowrates. Single material characteristics, such as wettability, roughness and thermal properties cannot explain the observed CHF differences between test materials. Roughness and thermal effusivity are power and linear relationships related to HTC at low flowrate,

respectively. However, under flow boiling conditions, compared to wettability, roughness and thermal properties of materials, boiling performance may be mainly determined by the nucleation site size distribution at the micrometer and submicron levels [7, 8]. Serials of work of MIT reveal that parameters of nucleation site density, a product of the nucleation frequency by the growth time, and average radius of discrete bubbles determine the boiling process, which is influenced by surface properties and characteristics [9, 10].

Based on the abovementioned research, flow boiling experiments are performed under the condition of atmospheric pressure, 400 kg·m^-2·s^-1 mass flowrate, and 5 ± 1 K inlet subcooling with five materials of 304SS, Inconel600, Monel400, Zr4, and FeCrAl to study the material-sensitivity HTC and CHF. These materials are extensively used in nuclear reactors, such as 304SS for structure materials, Inconel600 and Monel400 for fuel elements, and Inconel600, Zr4, and FeCrAl for fuel claddings. The size of each material is 1×1×0.1 cm, and the cross-section of the rectangular channel is 1×3 cm. To analyze the evolution of bubbles during boiling processes, a trained Convolutional Neural Network (CNN) will be used to post-process high-speed camera data.

2. Experimental setup and material parameters

2.1. Flow boiling experimental devices

The flow boiling experimental loop devices are shown in Figure 1. The loop mainly includes the following components: water tank, pump, filter, flow meter, preheating device, test section, chiller, and heat exchanger. The inlet and outlet temperature of the test section and the node temperature of the heating block are collected through thermocouples. Visual quartz glass windows are installed on the left and right sides and front of the test section. Through the visualization window, the formation, growth, and detachment of bubbles can be observed. A high-speed camera records the dynamic behavior of bubbles during boiling. The installation position of the copper heater and valve core is located behind the test section. A 1 mm thick heating element is welded to the copper heater through Zn-Al-Cu solder to reduce contact thermal resistance as much as possible. A LabVIEW interface is used to record the temperatures and voltage signals.

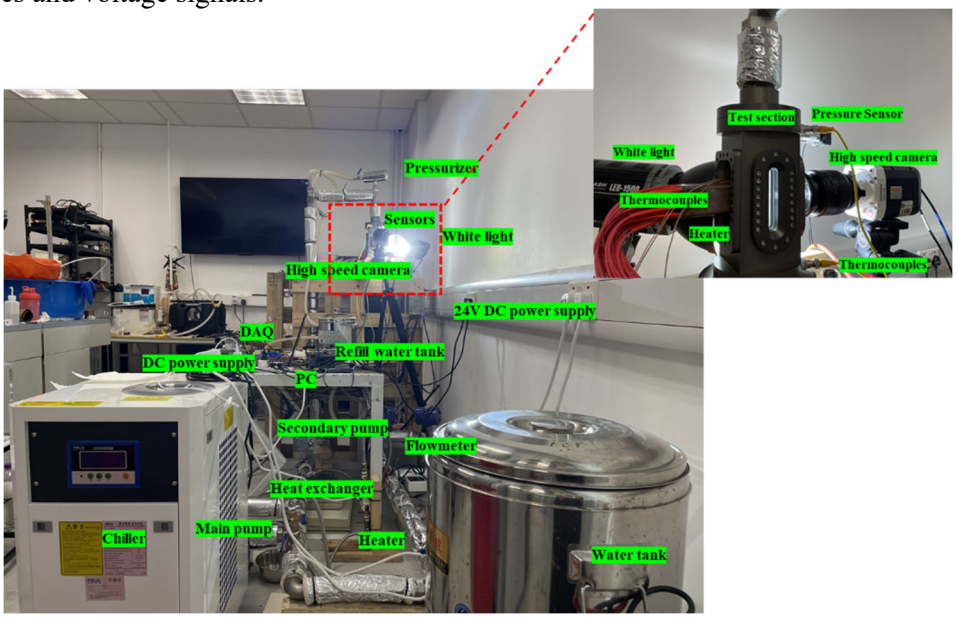

Figure 1. Flow boiling experiment devices.

The experimental procedures are divided into preheating, degassing, and boiling. A 2200W preheating device is used to increase the temperature of the deionized water in the loop and degas it. Then, continue heating until the tiny bubbles in the loop disappear. Before starting a flow boiling experiment, the flow rate of the loop and inlet temperature of the tested section recorded by the DAQ

stabilized at around 400 kg·m^-2·s^-1 and 95 °C, respectively. The heat flux is adjusted by changing the applied voltage of the dry-burning rods. The voltage rise interval is 5V. Once CHF is reached, the power is immediately turned off to prevent the heating element from burning.

Heat flux, wall superheat and HTC are calculated by the following equations:

$$q = -\lambda_{Cu}\frac{dT}{dx} = -\lambda_{Cu}\left(\frac{3T_1 - 4T_2 + T_3}{2\Delta x}\right) \quad (1)$$

$$T_s = (T_1 - q \times 1000 \times (\Delta x_{cu} / \lambda_{cu} + \Delta x_{\text{solder}} / \lambda_{solder} + \Delta x_{metal} / \lambda_{metal})) - 100 \quad (2)$$

$$HTC = q / (T_s + 100 - 0.5 \times (T_{in} + T_{out})) \quad (3)$$

where, q is heat flux, λ is thermal conductivity, T_1, T_2 and T_3 are temperatures measured by thermocouples at an equal interval, Δx is the interval, T_s is wall superheat, HTC is heat transfer coefficient, T_{in} and T_{out} are inlet and outlet temperatures, respectively.

2.2. Material thermo-physical and surface properties

Table 1 shows the thermo-physical properties of each material. Contact angle measurement instruments and an optical surface profilometer are used to measure wettability and roughness, as shown in Figure 2.

Table 1. Material thermo-physical properties.

Materials	Thermal conductivity (W/m/K)	Thermal effusivity ($J/s^{1/2}\cdot m^2\cdot K$)
304SS	15.0	7876.6
Inconel600	15.1	7792.3
Monel400	25.5	10071.2
FeCrAl	13.8	7374.8
Zr4	15.3	5393.2
ZnAlCu	76	-

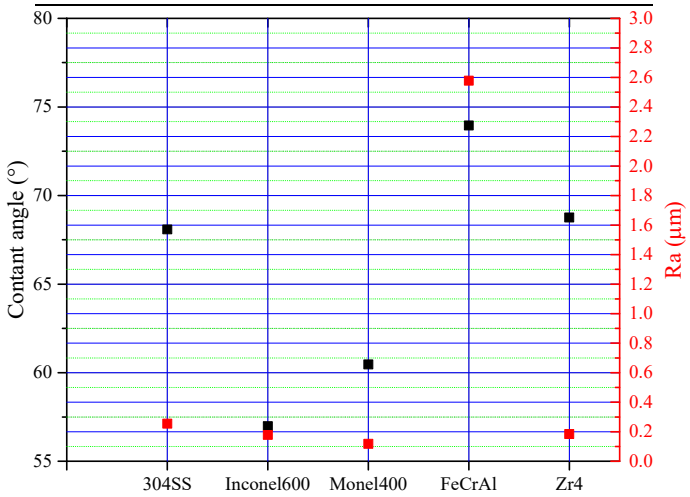

Figure 2. Wettability and roughness of each material.

Except for FeCrAl, arithmetic mean height Ra ranges from 0.1179 to 0.3735 μm. The difference in roughness represents the difference in nucleation site density. The 2.578 μm Ra of FeCrAl is much higher than other materials due to surface wavy wrinkles. This means the nucleation site density of

FeCrAl is much larger than other materials. All materials are hydrophilic, and the maximum contact angle difference between FeCrAl and Inconel600 is about 17°. The relatively small difference in wettability between these materials can provide a more intuitive material difference, which can help analyze differences in boiling performance caused by differences in material surface structure.

3. Results and discussion

The boiling curves of all selected materials are shown in Figure 3. Note that the tested materials can be divided into three groups according to difference in HTC even though their roughness and wettability are different, namely 304SS and Monel400; Inconel600; FeCrAl and Zr4.

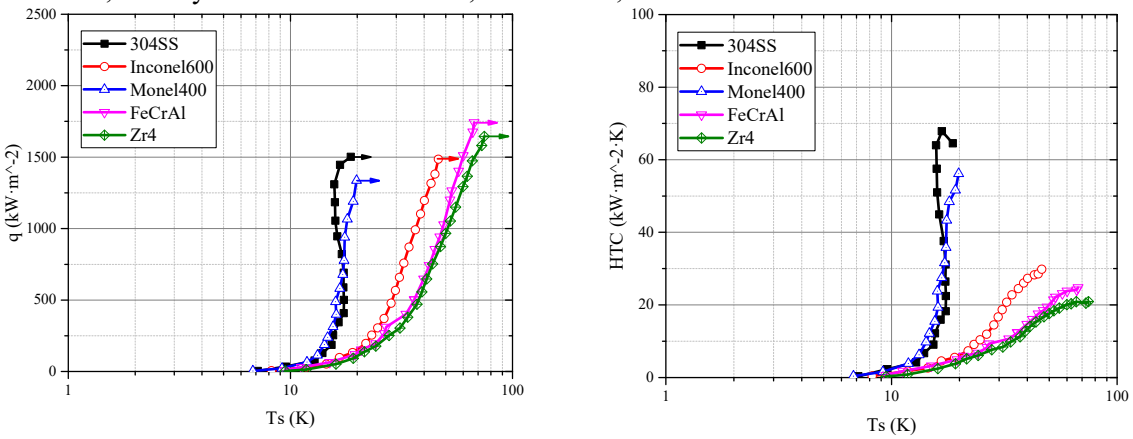

Figure 3. Flow boiling curves (a) and heat transfer coefficients (b) of tested materials.

Figure 4 shows changes in measured CHFs along with roughness and wettability, respectively. Even if CHF seems to increase with roughness and contact angle, a similar roughness or wettability level leads to various CHFs, such as Inconel600 and Zr4 for roughness, 304SS and Zr4 for wettability. Therefore, these discrepancies mean that single surface characteristics cannot provide an acceptable explanation for the HTC and CHF differences. CHF is a complex phenomenon that is difficult to predict based on just one material parameter. Wettability and roughness are also good indicators to predict CHF qualitatively and quantitatively, especially for evaluating CHF value for a specific material, while nucleation site size and distribution on a surface may provide a more intuitive CHF evaluation because they can determine the nucleation site density and area.

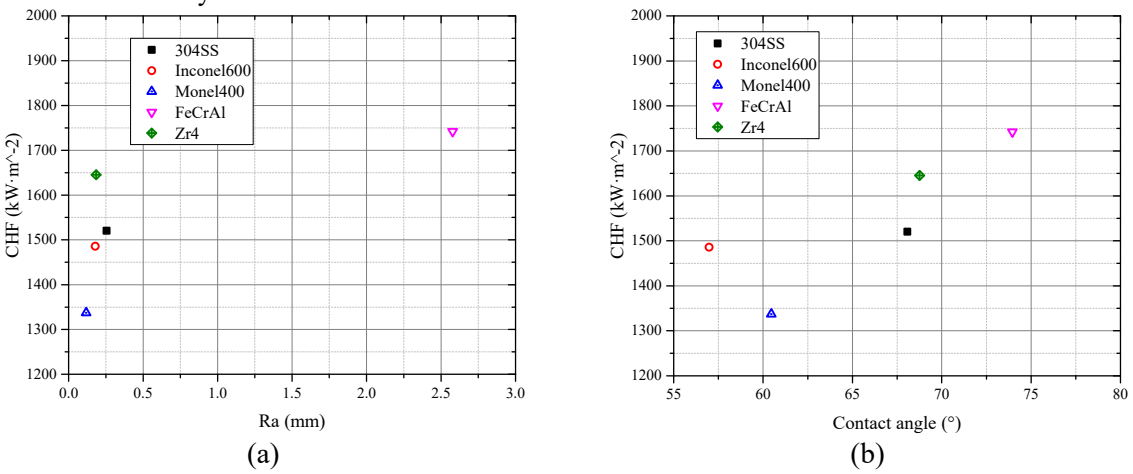

Figure 4. Measured CHFs of different materials relative to the (a) roughness and (b) wettability.

According to the mechanism of bubble congestion near the wall, bubbles formed on the wall are not easily diffused rapidly at lower mass flow rates, leading to the occurrence of CHF phenomenon. Nucleation site density and the minimum bubble nucleation area are focused on exploring the material-

sensitivity CHF mechanism and are presented in Figure 5. FeCrAl has the highest nucleation density due to its unique surface structure, which gradually decreases with increasing heat flux due to the coalescence of bubbles. Nucleation site densities of other tested materials increase first and then decrease as the heat flux density increases. All tested materials have a similar nucleation site density level at about 250 kW·m^-2. This is because partially active nucleation sites are covered by large bubble clusters. Figure 5 (b) shows each tested material's minimum bubble nucleation area. It can be seen that a higher CHF is relative to a smaller bubble nucleation area.

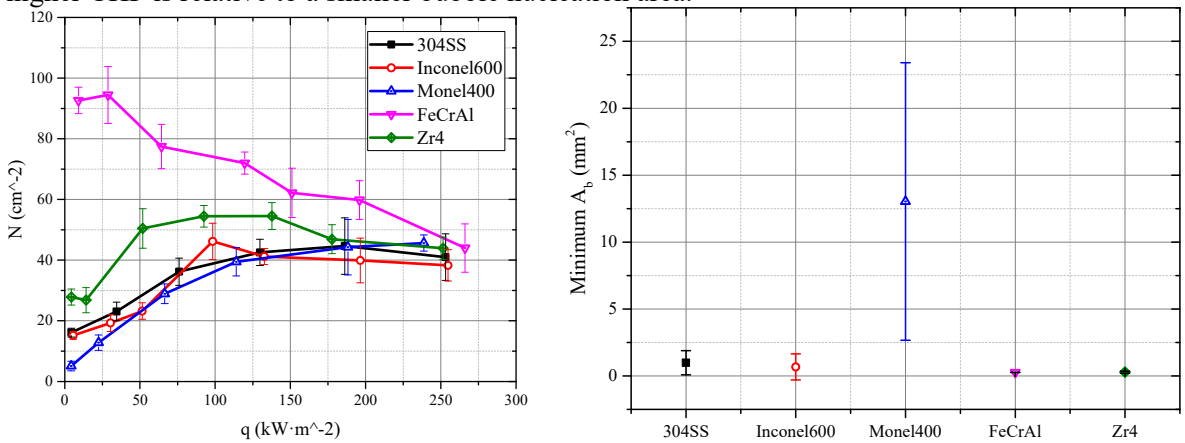

(a) (b)

Figure 5. Boiling parameters of tested materials relevant to the (a) nucleation site density and (b) minimum bubble nucleation area.

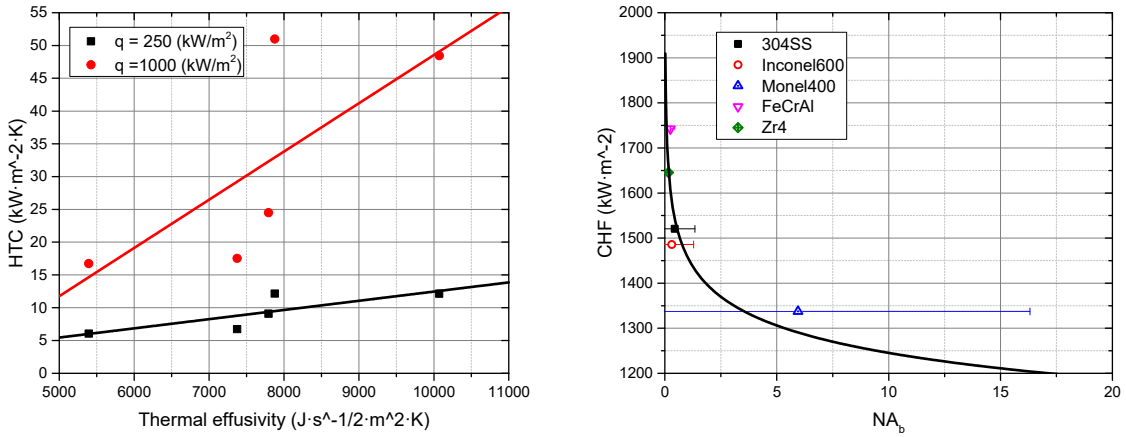

(a) (b)

Figure 6. Material-sensitive properties of (a) HTC and (b) CHF.

Thermal effusivity is also linearly related to HTC in our works, as shown in Figure 6 (a). One possible reason why the HTC curves of 304 SS and Mone1400 and those of FeCrAl and Zr4 are closer is that the thermal effusivity dominates the HTC. However, surface roughness only slightly affects HTC, especially for high heat flux conditions. Therefore, it can be seen that the HTC of 304 SS is close to Monel 400 but slightly higher at the same superheat level due to higher roughness, which is the same as FeCrAl and Zr4. A dimensionless parameter of the product of the maximum nucleation site density and the minimum bubble nucleation area is proposed in Figure 6 (b). CHF shows a power relationship to the dimensionless parameter, indicating that CHF is a scale-free phenomenon. Thus, material-sensitive CHF may be due to differences in the density of active nucleation sites and the area of nucleation bubbles.

This means that surface structure of material controls the nucleation site density and the minimum bubble nucleation area to determine CHF value and thermal effusivity of material dominates the HTC.

4. Conclusion

In this study, steady-state vertical upward flow boiling experiments were conducted at atmospheric pressure with fixed inlet subcooling and mass flowrate. Five materials, involving 304SS, Inconel600, Monel400, Zr4 and FeCrAl, were used to investigate the influence of material on flow boiling performance and CHF. The tested materials exhibited different flow boiling curves and HTCs.

Surface roughness and wettability were measured to demonstrate the disordered effect on flow boiling behaviors. Material thermo-physical properties directly impact HTC, and thermal effusivity shows a linear relationship to HTC. The flow boiling CHF may be determined by nucleation site density and bubble nucleation area. This means that broader macroscopic or microscopic studies of flow boiling phenomena are needed to explain the sensitivity of materials to CHF.

References

[1] Chu H, Yu X, Jiang H, Wang D and Xu N 2023 *Int. J. Heat Mass Transfer* **200** 123530
[2] Li W, Dai R, Zeng M and Wang Q 2020 *Renewable Sustainable Energy Rev.* **130** 109926
[3] O'Hanley H, Coyle C, Buongiorno J, McKrell T, Hu L W, Rubner M and Cohen R 2013 *Appl. Phys. Lett.* **103** 024102
[4] Paz M C , Conde M , Suárez E and Concheiro M 2015 *Exp. Therm Fluid Sci.* **64** 114-124
[5] Lee S K, Liu M, Brown N R, Terrani K A, Blandford E D, Ban H, Jensen C B and Lee Y 2019 *Int. J. Heat Mass Transfer* **132** 643-654
[6] Lee S K, Lee Y, Brown N R and Terrani K A 2020 *Int. J. Heat Mass Transfer* **158** 119970
[7] Seong J H, Wang C, Phillips B and Bucci M 2022 *Appl. Therm. Eng.* **213** 118670
[8] Seong J H, Wang C, Phillips B and Bucci M 2022 *Int. J. Heat Mass Transfer* **188** 122620
[9] Zhang, L, Seong, J H, Bucci, M 2019 *Phys. Rev. Lett.* **122** 134501
[10] Zhang, L, Wang, C, Su, G, Kossolapov, A, Matana Aguiar, G, Seong, J H, Chavagnat, F, Phillips, B, Rahman, M M, Bucci, M 2023 *Nat. Commun.* **14** 2321